Cell Reports, Volume *39*

Supplemental information

G6PD inhibition sensitizes ovarian cancer cells to oxidative stress in the metastatic omental microenvironment

Shree Bose, Qiang Huang, Yunhan Ma, Lihua Wang, Grecia O. Rivera, Yunxin Ouyang, Regina Whitaker, Rebecca A. Gibson, Christopher D. Kontos, Andrew Berchuck, Rebecca A. Previs, and Xiling Shen

Supplementary Figures

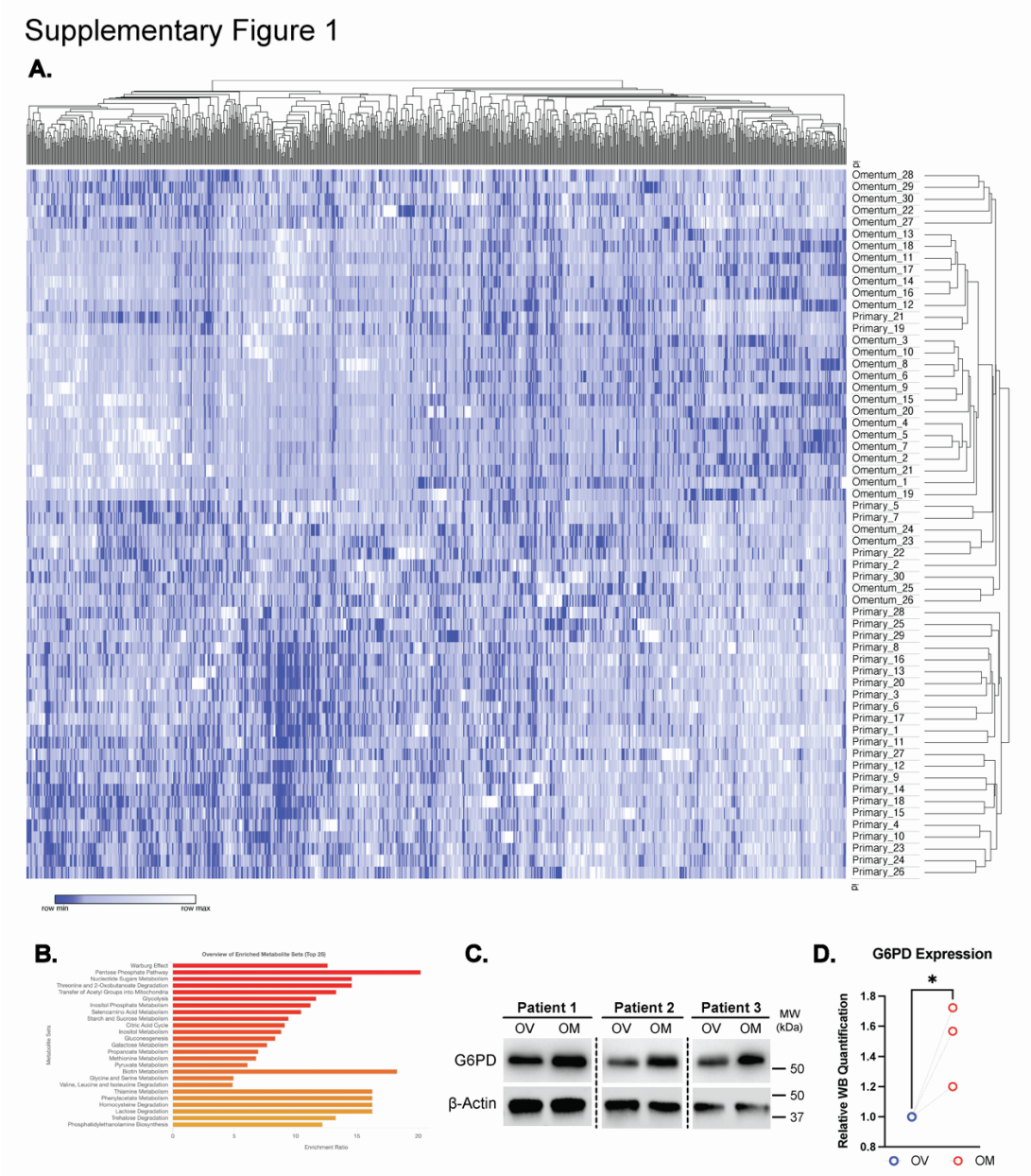

Figure S1: Gene expression and metabolomics analysis highlight PPP changes in matched human ovarian and omental tumors, Related to Figure 1. (A) Hierarchical clustering of heatmap of metabolic gene expression data from ovarian and omental tumors (n=30) show clustering of primary tumors and metastatic tumors independently. **(B)** Pathway analysis of metabolite abundance differences from LC-MS metabolomics analysis of matched primary ovarian tumor vs. omental metastases (n=8) highlight the pentose phosphate pathway. **(C)** Immunoblotting for G6PD in ovarian and omental tumors (n=3). **(D)** Quantification was performed by normalizing protein expression to the loading β-actin control and the primary tumor expression. Omental metastases exhibited increased G6PD expression (p-val<0.05, Student's *t*-Test).

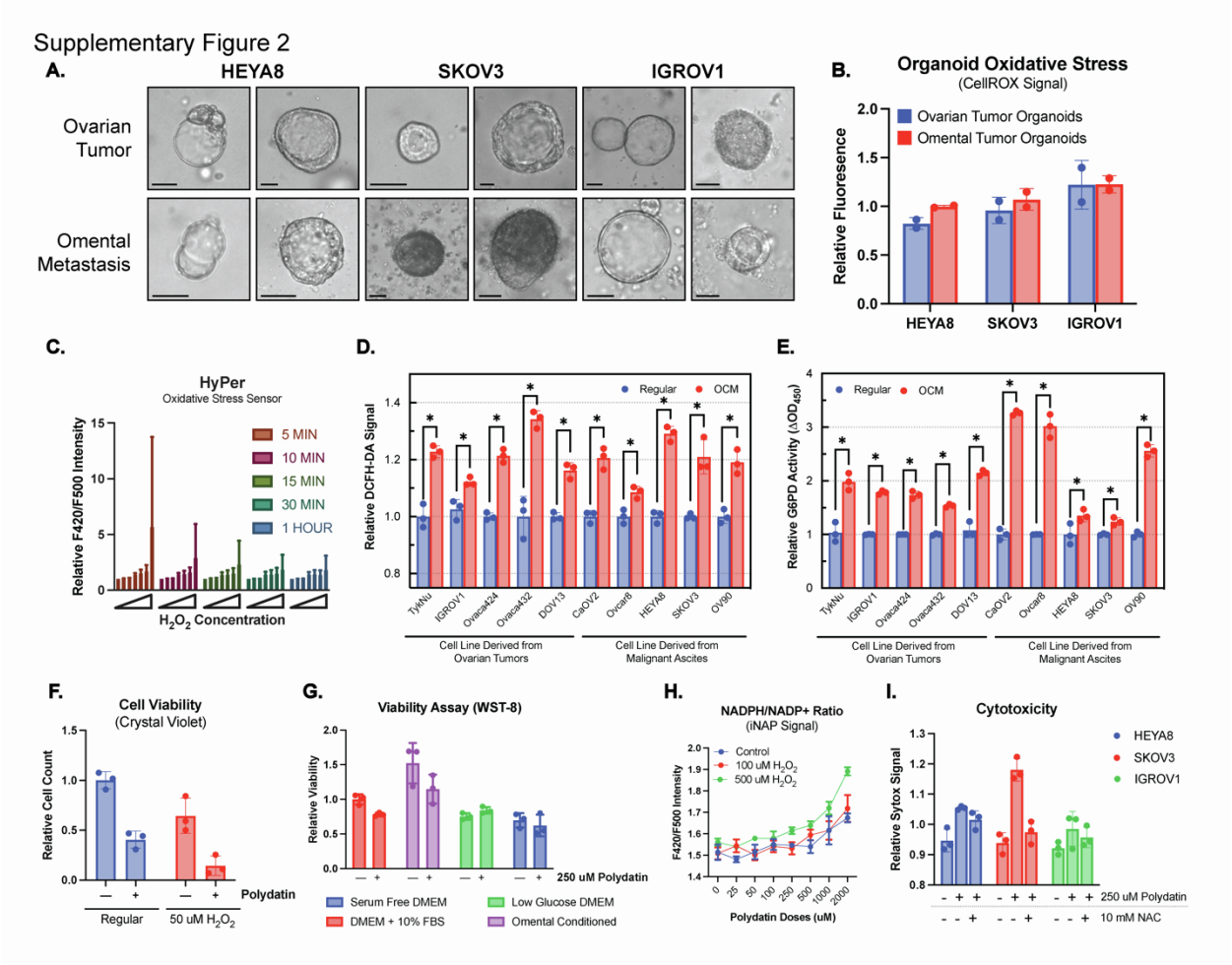

Figure S2: *In vitro* models of OC reflect changes in oxidative stress, Related to Figure 3. (A) Organoids were derived from murine ovarian tumors and omental metastases (n=2 per cell line). Scale bars represent 100 μM. **(B)** Oxidative stress of organoids cultured in organoid media measured using CellROX reveal minimal differences (n=2). **(C)** Fluorimetry of OC cells expressing HyPer was responsive to hydrogen peroxide exposure (n=3). Growth in OCM induced increases in **(D)** oxidative stress as measured via DCFH-DA incubation (n=3) and **(E)** G6PD activity as measured via enzymatic assay in 10 OC cell lines (n=3). **(F)** Crystal Violet and **(G)** WST-8 cell viability assays revealed less viable cells evident in OCM-polydatin treated samples (n=3). **(H)** iNAP fluorescence revealed increased NADPH/NADP+ in cells treated with polydatin (n=3). **(I)** N-acetylcysteine (NAC) treatment reversed these cytotoxic effects *in vitro* (n=3). The sample size (n) represents the number of technical replicates. Where indicated, statistical significance is noted using * p<0.05, ** p<0.01 by two-tailed Student's *t*-Test.

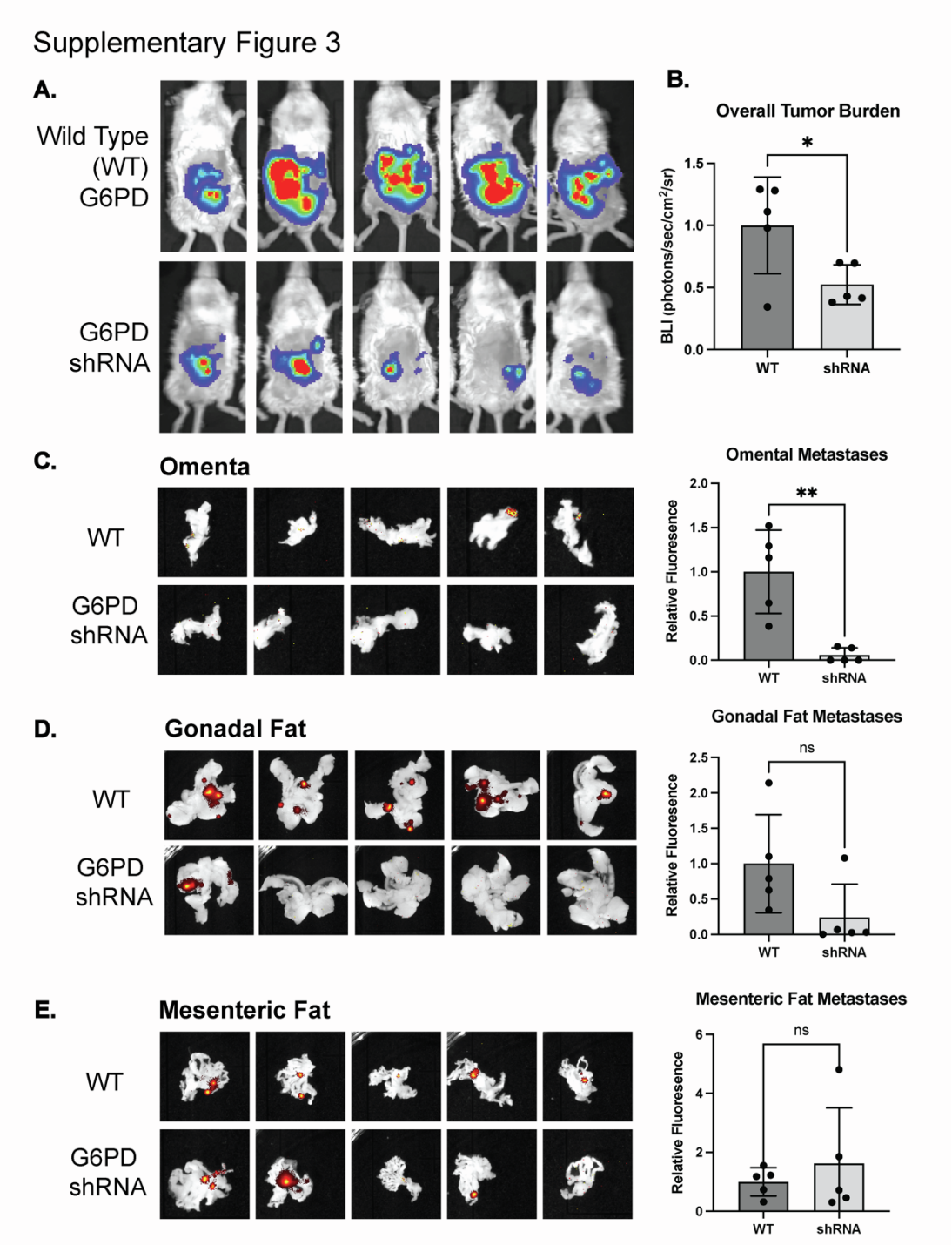

Figure S3: G6PD-shRNA knockdown reduces omental metastases *in vivo,* Related to Figure 4. (A) IVIS imaging and **(B)** quantification of tumor burden in NSG mice injected with wild-type and G6PD-shRNA expressing HEYA8-mCherry cells (n=5 per cohort). Fluorescence imaging and quantification of mCherry-expressing tumor burden in **(C)** omenta, **(D)** gonadal, and **(E)** mesenteric fat deposits (n=5 per cohort).

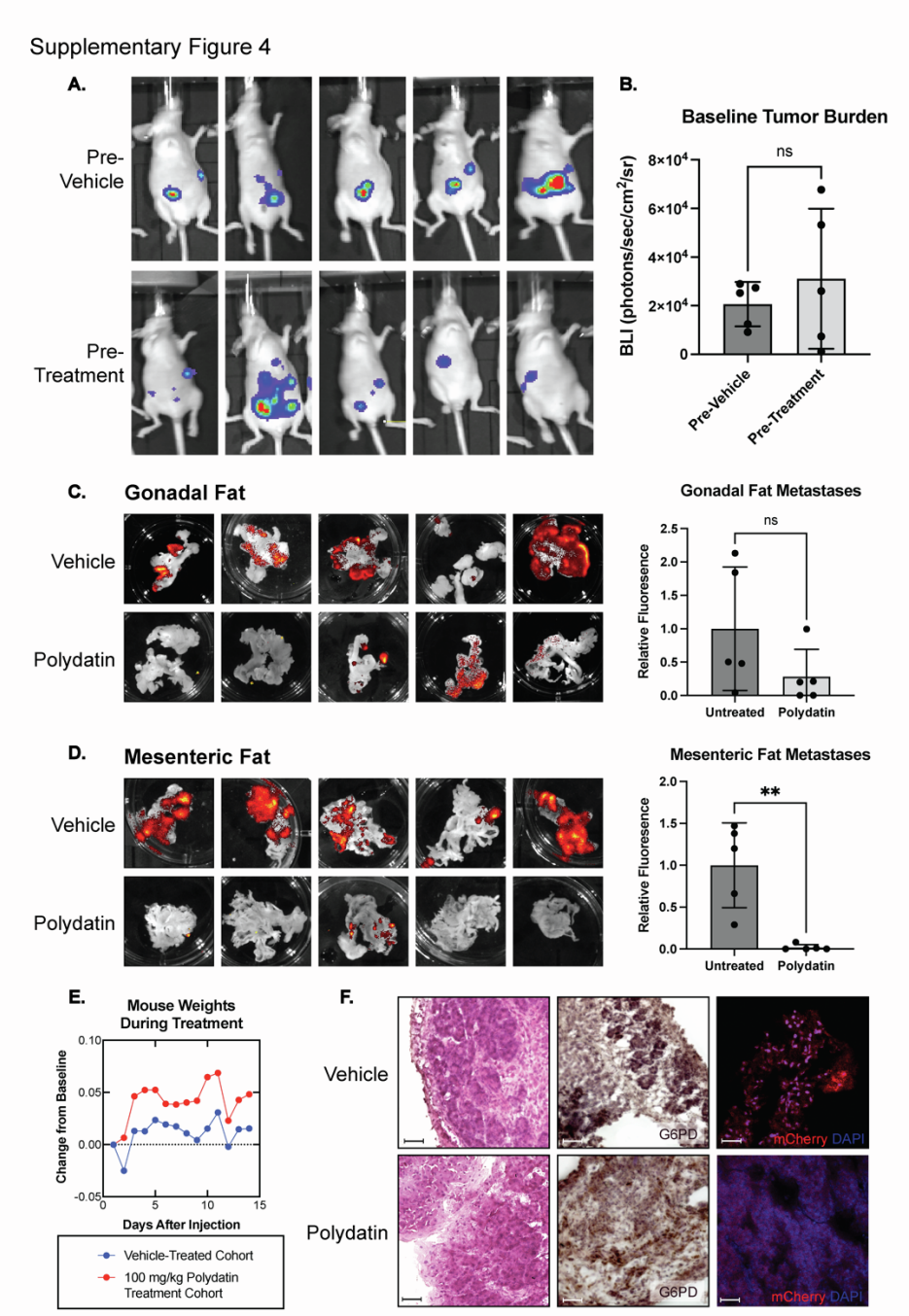

Figure S4: High-dose polydatin treatment (100 mg/kg) reduces mesenteric metastases *in vivo,* Related to Figure 4. (A) IVIS imaging and **(B)** quantification of baseline tumor engraftment taken 3 days post-injection of HEYA8-mCherry injected mice (n=5 per cohort). Fluorescence imaging and quantification of mCherry-expressing tumor burden in **(C)** gonadal and **(D)** mesenteric fat deposits. **(E)** Weights of mice did not vary significantly during course of treatment (each symbol is average of 5 mice per cohort, no statistically significant differences seen). **(F)** H&E, G6PD staining, and mCherry microscopy of omental tumors revealed similar tumor morphology between vehicle and polydatin treated tumors. Scale bars represent 100 μM.

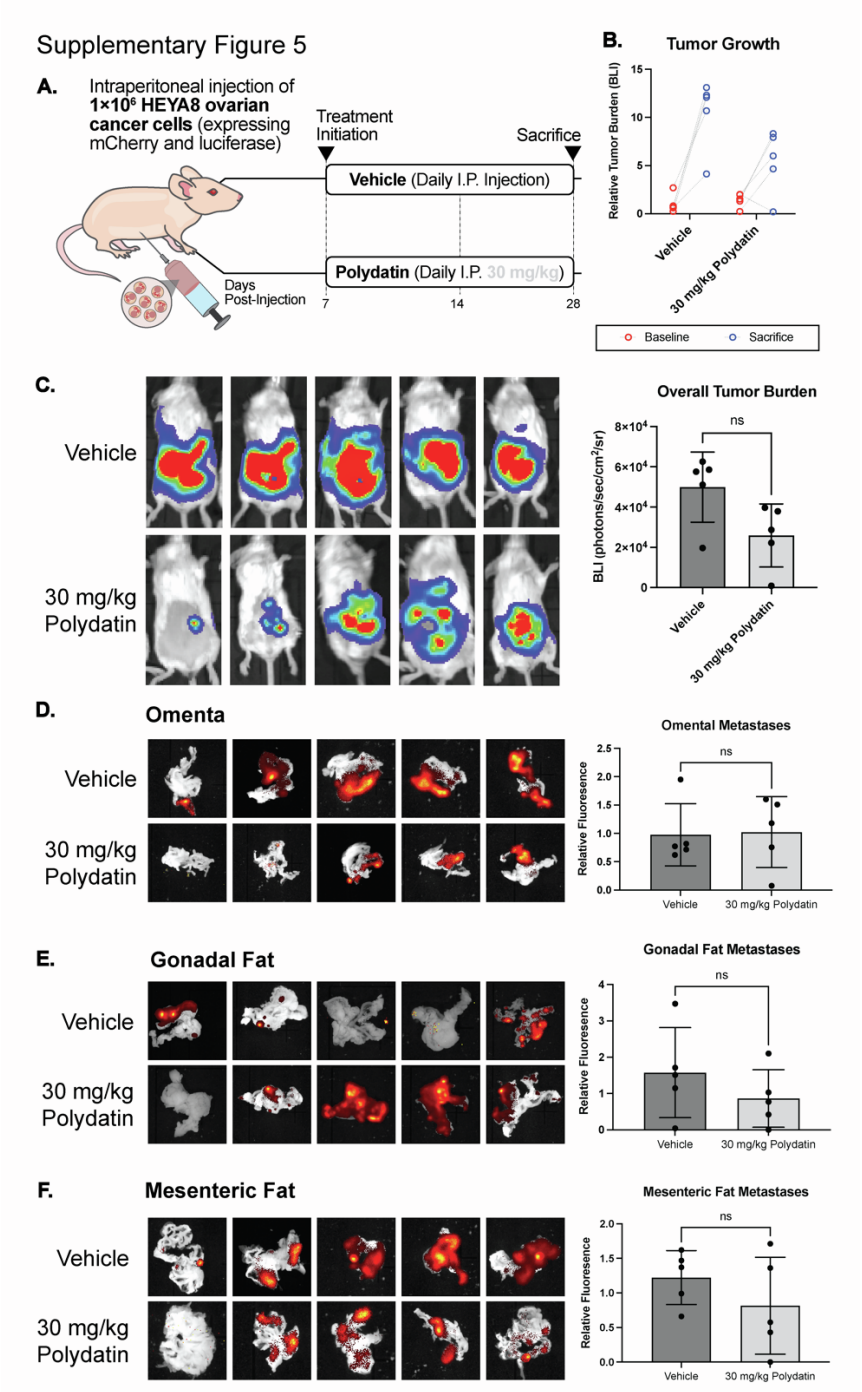

Figure S5: Low-dose polydatin (30 mg/kg) treatment does not dose not achieve therapeutic threshold *in vivo,* Related to Figure 4. (A) Schema for treatment. **(B)** Bioluminescence (BLI) was measured at baseline and prior to sacrifice using IVIS (n=5 per cohort). **(C)** IVIS imaging and BLI quantification prior to sacrifice shows tumor burden in 30 mg/kg polydatin treated and vehicle treated mice (n=5 per cohort). Fluorescence imaging and quantification of mCherry-expressing tumor burden in **(D)**

omenta, **(E)** gonadal, and **(F)** mesenteric fat deposits (n=5 per cohort). Labels of n.s. indicate “not significant” (p-val>0.05)

Media Component	Final Concentration
DMEM/F12	
GlutaMax	1x
Penicillin/Streptomycin	100 U/mL
17-B-Estradiol	10 nM
A083-01	250 nM
B27 (without Vitamin A)	1x
EGF	50 ng/mL
HGF	10 ng/mL
IGF1	20 ng/mL
N2 Supplement	1x
N-Acetylcysteine	5 mM
Neuregulin I	10 ng/mL
Nicotinamide	5 mM
Noggin	100 ng/mL
R-Spondin 1	50 ng/mL
SB203580 (p38i)	1 uM
Y-27632	10 uM

Table S1: OC Organoid Media Composition, Related to STAR Methods.

Patient Number	Ovarian Tumor ID	Omental Tumor ID	FIGO Stage	Age
1	1579	1577	4	37
2	1716	1714	4	70
3	1844	1842	3C	67
4	1925	1924	4	73
5	3427	3428	3C	45
6	3454	3451	3C	57
7	3474	3475	3C	45
8	6053	6054	3C	68

Table S2: Information About Human Tumor Samples, Related to STAR Methods.